Cell PRESS
Cell Stem Cell
Article

PUMA Regulates Intestinal Progenitor Cell Radiosensitivity and Gastrointestinal Syndrome

Wei Qiu,[1] Eleanor B. Carson-Walter,[4] Hongtao Liu,[2] Michael Epperly,[3] Joel S. Greenberger,[3] Gerard P. Zambetti,[5] Lin Zhang,[2,*] and Jian Yu[1,*]
[1]Department of Pathology
[2]Department of Pharmacology
[3]Department of Radiation Oncology
University of Pittsburgh Cancer Institute, Hillman Cancer Center, University of Pittsburgh, 5117 Centre Avenue, Pittsburgh, PA 15213, USA
[4]Department of Neurosurgery, University of Rochester, 601 Elmwood Avenue, Rochester, NY 14642, USA
[5]Department of Biochemistry, St. Jude Children's Research Hospital, 332 N. Lauderdale, Memphis, TN 38105, USA
*Correspondence: yuj2@upmc.edu (J.Y.), zhanglx@upmc.edu (L.Z.)
DOI 10.1016/j.stem.2008.03.009

SUMMARY

Radiation is one of the most effective cancer treatments. However, gastrointestinal (GI) syndrome is a major limiting factor in abdominal and pelvic radiotherapy. The loss of crypt stem cells or villus endothelial cells has been suggested to be responsible for radiation-induced intestinal damage. We report here a critical role of the BH3-only protein p53 upregulated modulator of apoptosis (PUMA) in the radiosensitivity of intestinal epithelium and pathogenesis of GI syndrome. PUMA was induced in a p53-dependent manner and mediated radiation-induced apoptosis via the mitochondrial pathway in the intestinal mucosa. PUMA-deficient mice exhibited blocked apoptosis in the intestinal progenitor and stem cells, enhanced crypt proliferation and regeneration, and prolonged survival following lethal doses of radiation. Unexpectedly, PUMA deficiency had little effect on radiation-induced intestinal endothelial apoptosis. Suppressing PUMA expression by antisense oligonucleotides provided significant intestinal radioprotection. Therefore, PUMA-mediated apoptosis in the progenitor and stem cell compartments is crucial for radiation-induced intestinal damage.

INTRODUCTION

Gastrointestinal toxicity is the primary limiting factor in abdominal and pelvic radiotherapy. Mice that receive greater than 14 Gray (Gy) die between 7 and 12 days due to damage to the small intestine and complications known as gastrointestinal (GI) syndrome (Komarova et al., 2004; Potten, 2004). The molecular determinants of intestinal radiosensitivity and GI syndrome are not well understood. Some believe that damage to stem cells plays a critical role in this process (Ch'ang et al., 2005; Potten, 2004). However, their precise location and characteristics had been elusive due to lack of definitive molecular markers. Many earlier studies suggested that putative stem cells reside at the cell position 4–6 immediately above Paneth cells (Giannakis et al., 2006; Potten, 2004; Stappenbeck et al., 2003). However, recently, genetic evidence convincingly showed that the columnar cells at crypt base (CBCs) that intermingled with Paneth cells are intestinal stem cells and suggest the cells at position 4–6 as progenitor cells (Barker et al., 2007). Several pathways have been implicated in regulating radiation-induced apoptosis in the crypt cells, including those of the tumor suppressors p53 and ATM (Ch'ang et al., 2005). p53 deficiency blocks early apoptosis in the crypt, occurring 3–6 hr following radiation, but leads to accelerated GI syndrome and animal death (Komarova et al., 2004; Merritt et al., 1994). The key mediator of p53-dependent apoptosis in this system has yet to be identified despite a long list of possible candidates (Potten, 2004; Yu and Zhang, 2005).

Others believe that endothelial apoptosis, which is independent of p53, is involved in the pathogenesis of GI syndrome, and suggest that the radiation-targeted cells switch from endothelial cells to epithelial cells at higher doses of radiation (Ch'ang et al., 2005; Paris et al., 2001). In this model, acid sphingomyelinase (ASMase)-mediated ceramide production was suggested to be responsible for apoptosis either in endothelial cells (lower than 18 Gy) or epithelial cells (higher than 18 Gy). Systemic administration of basic fibroblast growth factor, capable of suppressing ASMase in the endothelial cells, or deficiency in ASMase protected the murine small intestine from radiation-induced damage (Ch'ang et al., 2005; Paris et al., 2001).

We and others identified PUMA (p53 upregulated modulator of apoptosis) as a BH3-only Bcl-2 family protein that plays an essential role in p53-dependent and -independent apoptosis (Yu et al., 2001; Nakano and Vousden, 2001; Han et al., 2001). PUMA deficiency blocks apoptotic responses to p53 activation, DNA-damaging agents, and hypoxia in various tissue and cell types, including human cancer cells, mouse thymocytes, embryonic fibroblasts (MEFs), hematopoietic cells, and developing neurons (Yu et al., 2003; Jeffers et al., 2003; Villunger et al., 2003; Erlacher et al., 2005). Upon transcriptional induction in response to DNA damage, PUMA functions through other Bcl-2 family members, including Bax, Bcl-2, and Bcl-xL, to induce mitochondrial dysfunction and caspase activation (Yu et al., 2003, 2007; Ming et al., 2006; Wang et al., 2007).

In this study, we report a critical role for PUMA-mediated apoptosis in the radiosensitivity of intestinal progenitor and stem cell compartments and the pathogenesis of GI syndrome. We found that p53-dependent PUMA induction is largely

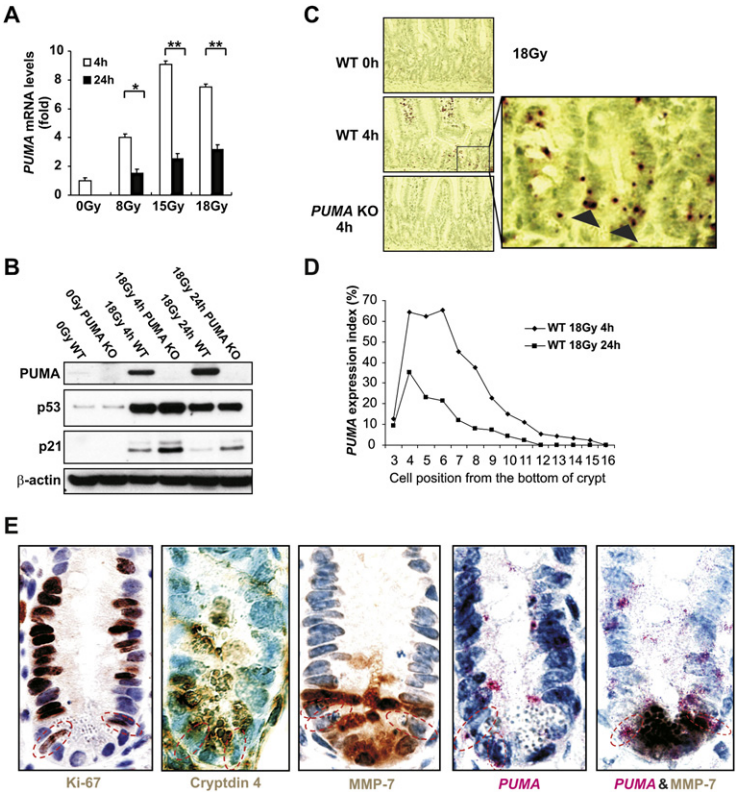

Figure 1. Radiation Induced Intestinal PUMA Expression

(A) *PUMA* mRNA expression in the jejunal mucosa of mice following whole body radiation (WRB) was evaluated by quantitative real-time RT-PCR. Values are means ± SD; n = 3 in each group. *p < 0.01; **p < 0.001.

(B) PUMA, p53, and p21 protein expression in the jejunal mucosa of mice with indicated genotypes was determined by western blotting. β-actin was used as the control for loading.

(C) *PUMA* mRNA in situ hybridization (ISH) in the jejunum of mice following radiation (magnification ×400). The selected area is shown at a higher magnification. Arrows indicate examples of *PUMA*-expressing cells.

(D) *PUMA* mRNA expression (ISH) in the crypts was scored according to the cell position, pooled from 2 mice in each group.

(E) *PUMA* expression in the columnar cells at the crypt base (CBCs) at 4 hr after 18 Gy. Examples of the CBCs are circled in red and stained positive for Ki-67 but negative for Paneth cell markers cryptdin 4 and MMP-7, magnification ×600.

responsible for radiation-induced apoptosis in the intestinal progenitor and stem cells. PUMA deficiency resulted in enhanced crypt regeneration and prolonged survival of mice following lethal doses of radiation. Despite a rapid induction of PUMA by radiation in the intestinal endothelial cells, its ablation had virtually no effect on their apoptosis. Our data suggest that targeting PUMA may be therapeutically useful to manipulate the radiation responses in cancer patients.

RESULTS

Radiation Rapidly Induced Intestinal PUMA Expression

PUMA expression in the intestinal mucosa of wild-type (WT) mice was examined by real-time RT-PCR and western blotting. *PUMA* mRNA was induced by 4-, 9-, and 7-fold at 4 hr after 8, 15, and 18 Gy of whole-body radiation (WBR), respectively (Figure 1A). The induction decreased by more than 60% by 24 hr and almost disappeared by 48 hr (Figure 1A; data not shown). PUMA protein expression was elevated at 4 hr and continued to increase at 24 hr (Figure 1B). RNA in situ hybridization (ISH) indicated strong staining of *PUMA* mRNA in the crypts 4 hr after 18 Gy radiation, which decreased significantly at 24 hr (Figure 1C). PUMA staining was primarily localized to the lower part of the crypt, both in the cells at positions 4–6 (Figures 1C and D) and in the columnar cells at crypt base (CBCs) (Figure 1E and Figure S1A). The CBCs stained positive for the proliferation marker Ki-67 but negative for Paneth cell marker cryptdin 4 or MMP-7 (Barker et al., 2007). We also noticed that some +4 cells appear intermingled with Paneth cells (Figure 1E and Figure S1A). Similar results were obtained from mice received 15 Gy WBR (data not shown). These results indicate that radiation rapidly induced PUMA mRNA and protein expression in the progenitor and stem cell compartments of the small intestine.

PUMA Deficiency Impaired Radiation-Induced Apoptosis in the Intestinal Progenitor and Stem Cells

Radiation (18 Gy) induced marked apoptosis in the crypt of WT mice, which was blocked by 90% and 80% at 4 and 24 hr in *PUMA* KO mice, respectively (Figures 2A and 2B). The DNA laddering in the intestinal mucosa and apoptosis of villus epithelial cells were also significantly suppressed in *PUMA* KO mice (Figures S1B and S1C). More specifically, apoptosis at the cell positions 4–6 was blocked by 92% and 66% in *PUMA* KO mice at 4 and 24 hr, respectively (Figures 2C and 2D). Notably, in WT animals, *PUMA* mRNA was highly expressed in the apoptotic cells identified by the putative progenitor marker Musashi (Figures 2E and 2F) (He et al., 2007; Potten et al., 2003). The putative progenitor cells in WT mice are highly sensitive to radiation-induced apoptosis, and more than 95% crypts contained apoptotic cells at positions 4–9 following 8, 15, or 18 Gy (Figure 2A; Figures S2B and S3B). In contrast, the CBCs are more resistant to radiation-induced apoptosis (Barker et al., 2007), with the fraction of crypts containing apoptotic CBCs at 10%, 27.5%, and 35% after 8, 15, and 18 Gy in WT mice, respectively (Figures 2G and 2H). PUMA deficiency also blocked apoptosis in the CBCs by at least 50% at 4 and 24 hr (Figure 2H). These results demonstrate that PUMA is an important mediator of radiation-induced apoptosis in the intestinal progenitor and stem cells.

PUMA Deficiency Did Not Affect Radiation-Induced Intestinal Endothelial Apoptosis

Several groups suggested the involvement of endothelial apoptosis in the pathogenesis of GI syndrome (Ch'ang et al., 2005; Paris et al., 2001). However, we found that radiation-induced apoptosis in the lamina propria of WT mice occurred to a similar degree at 4 hr following different doses of radiation (8, 15, and 18 Gy) and consistently decreased by over 80% at 24 hr (Figures 3A

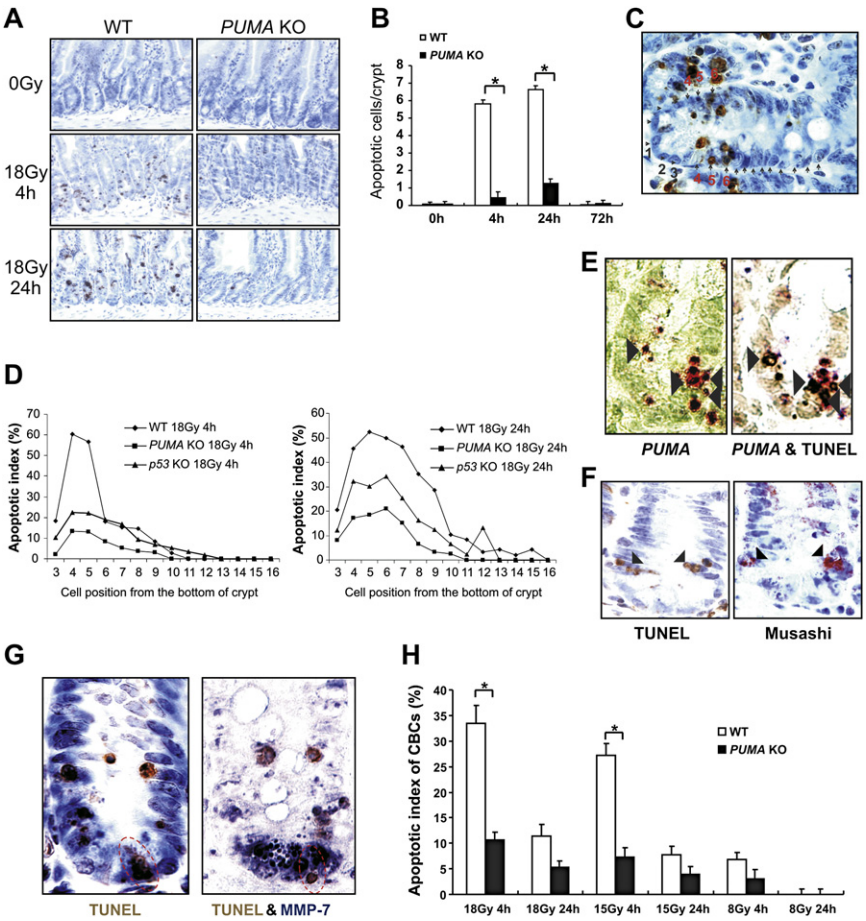

Figure 2. PUMA Mediated Radiation-Induced Apoptosis in the Intestinal Progenitor and Stem Cells

(A) Apoptosis in the small intestinal crypts at 4 hr and 24 hr after 18 Gy WBR was assessed by TUNEL staining (brown), magnification ×400.

(B) Apoptotic index in the crypts measured by TUNEL staining. Values are means ± SD; n = 3 in each group. *p < 0.005.

(C) Example of apoptotic cells and their position in the crypt at 4 hr following 18 Gy WBR, magnification ×1000. Paneth cells are indicated with arrowheads while non-Paneth cells are indicated by arrows.

(D) Apoptotic index at 4 hr (left panel) and 24 hr (right panel) following radiation. The apoptotic index was scored as the mean percentage of apoptotic cells of each cell position, pooled from four mice in each group.

(E) *PUMA* ISH, and *PUMA* ISH/TUNEL double staining in the crypts 4 hr after 15 Gy, magnification ×400. Arrows indicate double-positive cells.

(F) Serial sections (WT mice, 15 Gy at 4 hr) were subjected to TUNEL staining and Musashi IHC, magnification ×1000. Arrows indicate positive signals.

(G) Radiation-induced apoptosis in the CBCs. Sections were stained with TUNEL or TUNEL followed by MMP-7 IHC with several CBCs circled, magnification ×600.

(H) The fractions of crypts with at least one TUNEL-positive CBCs were calculated by counting 100 crypts with well preserved Paneth cell areas. Values are means ± SD; n = 3 in each group. *p < 0.005.

and 3B). Unexpectedly, apoptosis in this compartment was not affected in *PUMA* KO mice, despite a rapid and robust induction of *PUMA* by 4 hr in WT mice (Figure 3C and data not shown). Using an endothelial marker CD105 (endogolin; Ge and Butcher, 1994), we found that only a small percentage (less than 14%) of CD105-positive cells underwent apoptosis 4 hr after 18 or 15 Gy radiation, which decreased to less than 5% at 24 hr (Figures 3D–3F). Furthermore, neither the fraction of apoptotic CD105-positive cells nor the total number of CD105-positive cells following radiation was affected in *PUMA* KO mice (Figures 3F and G). The majority of apoptotic endothelial cells expressed *PUMA* (Figure 3J; Figures S4B and S4C). Apoptosis in the endothelial cells occurred soon (within 1 hr) after radiation (Figure 3H; Figure S4A) and led to an apparent reduction (30%–50%) in their numbers within 4 hr (Figures 3G and I). In addition, *PUMA* induction was more limited in other cell types, such as hematopoietic cells (19% of cells), compared with that in the endothelial cells (80%–85% of cells) (Figure S4D). The above data suggest that *PUMA* is rapidly and widely induced in the endothelial compartment of the small intestine following radiation but is not required for its apoptosis.

Radiation-Induced Intestinal Apoptosis Is Mediated through the Mitochondrial Pathway

To investigate the mechanisms of PUMA-mediated apoptosis following radiation, we analyzed several mitochondria-related events in the intestinal mucosa. Radiation induced cytosolic release of cytochrome c, mitochondrial translocation, and multimerization of Bax in WT mice, which were virtually blocked in *PUMA* KO mice (Figures 4A and 4B). As Bax and Bak have redundant functions in some cells (Zong et al., 2001), we also examined Bak translocation and multimerization. Bak multimerization was slightly reduced in the irradiated *PUMA* KO mice, while no change in Bak redistribution was detected (Figures 4A and 4B). Nevertheless, radiation-induced caspase 3 activities and processing were significantly blocked in *PUMA* KO mice (Figures 4C and D). Consistent with a role of Bax in PUMA-mediated apoptosis, *BAX* KO mice exhibited reduced crypt apoptosis (Figure 4E). These results collectively suggest that PUMA mediates radiation-induced intestinal apoptosis predominantly through Bax activation and the mitochondrial pathway.

PUMA Deficiency Resulted in Enhanced Crypt Regeneration and Prolonged Survival of Mice Following WBR

We reasoned that enhanced stem or progenitor cell survival in *PUMA* KO mice would lead to enhanced crypt proliferation and regeneration following radiation. Comparison of proliferation in the small intestine of WT and *PUMA* KO mice revealed no significant difference before or 4 hr after 18 Gy. However, there were twice as many BrdU-positive cells at 24 hr in *PUMA* KO mice (Figure 5A; Figure S5A). Microcolony assay was used to measure the regeneration capacity of stem cells at day 4 after 15 Gy

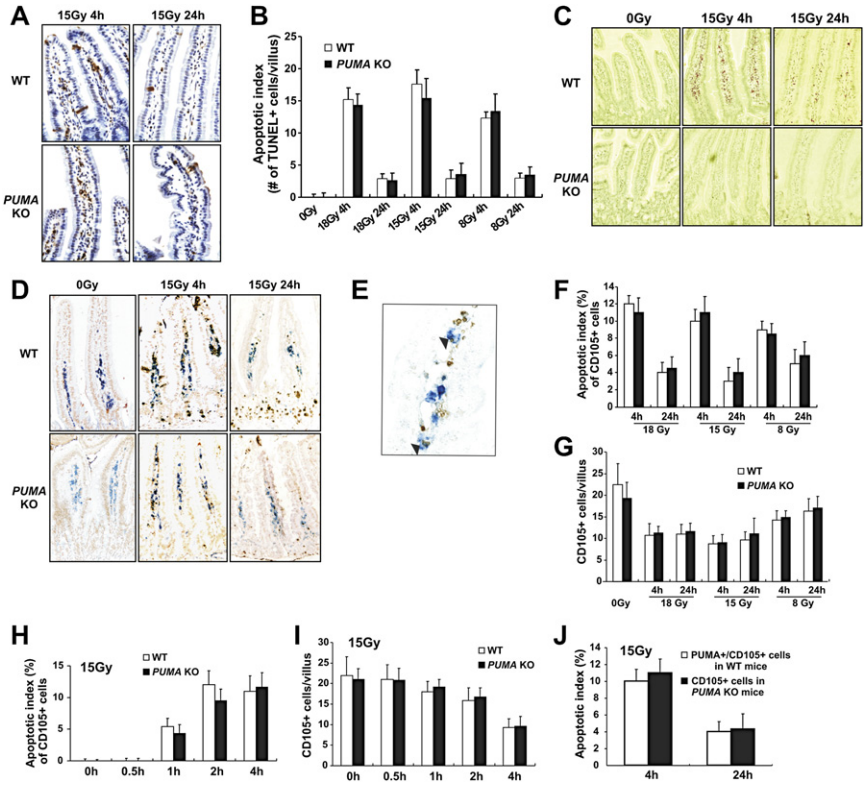

Figure 3. PUMA Did Not Contribute to Radiation-Induced Intestinal Endothelial Apoptosis

(A) Apoptosis induced by radiation in the villus was assessed by TUNEL staining (brown), magnification ×400.

(B) Apoptotic index in the villus submucosa. Values are means ± SD. n = 3 mice in each group.

(C) *PUMA* mRNA (red) ISH in the jejunal villi, magnification ×200.

(D and E) The sections were double stained with TUNEL (brown) and CD105 (blue), magnifications ×200 and ×1000, respectively. Arrows indicate double positive cells.

(F) The average fraction (%) of TUNEL+/CD105+ cells in the villus. Values are means ± SD; n = 3 mice in each group.

(G) The average number of CD105+ cells in the villus. Values are means ± SD; n = 3 mice in each group.

(H) Apoptotic index of CD105+ cells was determined at indicated times in WT and *PUMA* KO mice as in (F).

(I) The number of CD105+ cells were determined at indicated times as in (G).

(J) Apoptotic index of CD105+/*PUMA*+ cells in WT mice and that of CD105+ cells in *PUMA* KO mice were determined in 100 villi/mouse. Values are means ± SD; n = 3 mice in each group.

radiation. We found that crypt regeneration increased by nearly 100% in *PUMA* KO mice compared with that in WT mice (Figure 5B; Figure S5B). Crypt regeneration was also enhanced in *BAX* KO mice, though to a lesser extent than that in *PUMA* KO mice (Figure 5C). Since almost all crypts vanished at day 3 (Figure S5C), the crypts found on day 4 are likely to be formed "de novo" by radio-resistant stem cells (i.e., CBCs), which are devoid of Musashi expression (Figure S6). The intestinal epithelium completely recovered in both WT and *PUMA* KO mice at a lower dose of radiation (8 Gy) (Figure S7).

We then determined whether differences in crypt apoptosis and regeneration have an impact on animal survival. *PUMA* KO mice were found to survive approximately 50% longer than their wild-type counterparts after 15 Gy or 18 Gy WBR (Figure 5D). Drastic differences in the degree of intestinal injury were revealed by histological analysis (Figure 5E). A progressive reduction in the length of villi, culminating in their complete destruction, was evident in WT mice from 72 to 108 hr. Massive lymphocytic infiltration and thickening of the lamina propria below the base of the crypts suggested loss of intestinal epithelial integrity. However, the villus shortening and submucosal inflammation were significantly blunted in *PUMA* KO mice (Figure 5E). This probably explains why more than 80% of wild-type mice had died while 100% of *PUMA* KO mice were alive by 108 hr following 18 Gy WBR (Figure 5D). These data suggest that PUMA plays a critical role in the development of GI syndrome and the death of clonogenic stem cells following lethal doses of radiation.

p53 and Radiation-Induced Intestinal PUMA Expression

We then sought to determine whether p53 plays a role in radiation-mediated *PUMA* induction in the intestinal mucosa. The induction of *PUMA* mRNA and protein was found to be completely abrogated in *p53* KO mice (Figures 6A and 6B). Compared with WT mice, crypt apoptosis was reduced by 40% and 60% in *p53* KO mice at 4 and 24 hr following radiation, respectively (Figure 6C; Figure S8A). The early crypt apoptosis induced by 8 Gy radiation was blocked to a similar extent in *p53* KO and *PUMA* KO mice (Figures S9 and S3). In contrast to *PUMA* KO mice, *p53* KO mice exhibited a profound increase (2.3-fold) in crypt proliferation by 24 hr (Figures S8B and S8C) but only a slight increase in crypt regeneration with almost complete destruction of villi by 96 hr (Figure 6D; Figure S8D). Consistent with these pathological findings, *p53* KO mice died 3.5 days sooner than WT mice on average (Figure 5D; data not shown). Radiation can induce p53-independent apoptosis in some cells (Strasser et al., 1994). We therefore examined the expression of several other BH3-only proteins, including Bid, Bad, and Bim. Interestingly, none were induced by radiation in *p53* KO mice, while Bid and Bad were induced in WT mice (Figure S8E). These data suggest that p53-dependent PUMA induction is a key determinant of GI syndrome, and proteins other than the proapoptotic Bcl-2 members might contribute to the exacerbated GI syndrome found in *p53* KO mice.

PUMA Antisense Oligonucleotides Suppressed Intestinal Apoptosis and Prolonged Survival of Mice Following WBR

The above data imply that manipulation of PUMA expression is likely to provide intestinal radioprotection. To test this hypothesis, we first identified several *PUMA* antisense oligonucleotides (*PUMA* AS2 and AS3) that efficiently inhibited PUMA expression induced by Brefeldin A, an inhibitor of intracellular protein transport, in MEFs

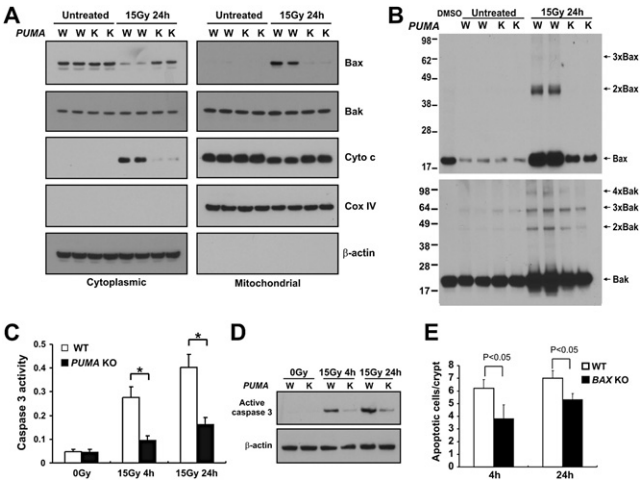

Figure 4. PUMA Mediated Radiation-Induced Intestinal Apoptosis via the Mitochondrial Pathway

(A) Bax, Bak, and cytochrome c (Cyto c) were analyzed in the cytosolic and mitochondrial fractions of intestinal mucosa by western blotting. β-actin and CoxIV were used as the controls for loading and fractionation.

(B) Formation of Bax and Bak multimers was analyzed in the chemical cross-linker DSP-treated mitochondrial fractions by western blotting under nondenaturing conditions.

(C) Caspase 3 activity was measured in the intestinal mucosa extracts. Values are means ± SD; n = 6 mice in each group. *$p < 0.01$.

(D) Caspase 3 processing and β-actin levels were analyzed by western blotting. Results of two representative animals from the treated groups are shown.

(E) Apoptotic index in the crypt was quantitated in WT and *BAX* KO mice after 15 Gy as in Figure 2B. Values are means ± SD; n = 3 mice in each group.

W, WT mice; K, *PUMA* KO mice.

(Table S1; Figure 7A). The two *PUMA* antisense oligos, but not a sense oligo, markedly inhibited intestinal PUMA expression induced by radiation and led to reduced crypt apoptosis, enhanced crypt proliferation, and regeneration (Figures 7B–7E; Figures S10A–S10D). The *PUMA* antisense oligos also increased the LD_{50} (number of days required to kill 50% of the animals) from 7 to 9 days (Figure 7F). These data indicate that PUMA inhibition provides significant intestinal radioprotection and prolongs survival.

DISCUSSION

The underlying molecular mechanisms of radiation-induced GI toxicity are largely unknown (Gudkov and Komarova, 2003; Komarova et al., 2004; Potten, 2004) despite their important implications in improving cancer treatment. In the current study, we showed that the BH3-only protein PUMA is a critical mediator of intestinal apoptosis induced by radiation predominantly via modulation of Bax activities. p53-dependent PUMA induction is mainly, if not solely, responsible for radiation-induced and p53-dependent early apoptosis in the intestinal progenitor cells. PUMA deficiency delayed GI syndrome and prolonged the survival of mice following lethal doses of radiation. To our knowledge, this is the first report in which deficiency in a single gene significantly protects against GI syndrome by preserving the progenitor and stem cell compartments and the structure and integrity of intestinal epithelium. The CBCs seem more resistant to the induction of apoptosis and *PUMA* following radiation compared with the cells at position 4–6 (Figures 1 and 2; Figures S1–S3). However, it is important to realize that our ability to detect the CBCs is still limited due to the fact that these long and slender cells are in close proximity to Paneth cells that are much more visually prominent. Therefore, the extent of apoptosis and *PUMA* expression in the CBCs might actually be higher. With the aid of a recently described intestinal stem cell marker and mouse models (Barker et al., 2007), future lineage tracing experiment should provide more definitive answers as to the genes and cellular compartment(s) involved in GI syndrome and crypt regeneration following radiation.

Our findings have several important implications. They provide a mechanistic explanation of intestinal radiosensitivity. Our study showed that PUMA was rapidly induced in both the progenitor and stem cell compartments in the small intestine and its ablation largely prevented their apoptosis within 24 hr (Figures 1 and 2; Figures S1–S3). *PUMA* ablation enhanced crypt proliferation and regeneration and preserved the intestinal integrity in a later phase (Figure 5). *PUMA* ablation had little effect on radiation-induced endothelial apoptosis despite its rapid induction in WT mice (Figure 3). Therefore, epithelial apoptosis, but not endothelial apoptosis, is the primary lesion in the rapid phase of radiation-induced intestinal damage as suggested by others (Hendry et al., 2001; Suit and Withers, 2001). Furthermore, our data fail to support the target switching model (Ch'ang et al., 2005; Paris et al., 2001), as endothelial apoptosis rapidly declined within 24 hr and was not affected by the doses of radiation (Figure 3). The discrepancy between our findings and those (Ch'ang et al., 2005; Paris et al., 2001) might be explained by the differences in the strains of mice and/or the doses of radiation and methods of detecting endothelial cells. It is possible that endothelial and epithelial apoptosis contribute to different aspects of GI death-associated syndrome, and the use of *PUMA* and *ASMase* double knockout mice might provide an answer.

The different responses of PUMA and p53-deficient mice provide an explanation for a seemingly paradoxical role of p53 in intestinal radiosensitivity. Our data strongly argue that PUMA is the primary, if not sole, mediator of p53-dependent apoptosis among all the proapoptotic p53 targets in the small intestine in response to radiation (Figures 1, 2, and 6) (Yu and Zhang, 2005). p53 and p21 deficiencies have been reported to accelerate GI syndrome and animal death (Komarova et al., 2004). It appears that p53-mediated p21 induction protects against GI syndrome while p53-mediated PUMA induction promotes GI syndrome (Figures 5 and 6). Interestingly, p21 levels were found to be significantly higher in the intestinal mucosa of *PUMA* KO mice after radiation (Figure 1B). One explanation is that p21-mediated cell-cycle arrest followed by DNA repair in the stem cell compartment is necessary for multiple rounds of successful cell division and ultimately crypt regeneration (Figures 5A and 5B). Therefore, it might be interesting to determine the intestinal radiosenstivity of mice deficient in both *PUMA* and *p21*. We would predict an even greater proliferative response, but less crypt regeneration following radiation in the double knockout mice than in *PUMA* KO mice. Future work is clearly needed to understand how cell death and proliferation are coordinated to regulate the intestinal stem cell regeneration following DNA damage or other clinically relevant insults.

Lastly, our data provides a rationale to target PUMA in GI syndrome. Several growth factors, including insulin growth factor

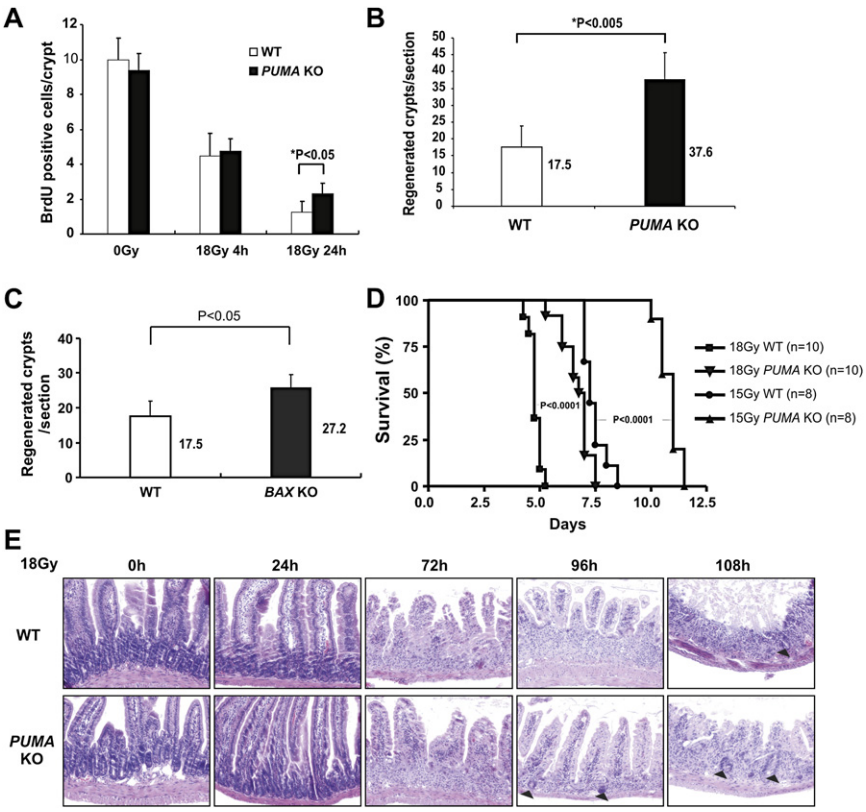

Figure 5. PUMA Deficiency Prolonged the Survival of Mice Following WBR

(A) BrdU incorporation index in the small intestine was quantitated by counting 100 crypts. Values are means ± SD; n = 3 mice in each group.

(B) Crypt regeneration was calculated by counting 10 cross-sections following BrdU staining. Values are means ± SD; n = 4 in each group.

(C) Regenerated crypts were quantitated in WT and *BAX* KO mice after 15 Gy WBR as in (B); n = 3 in each group.

(D) Survival curves of mice subjected to 15 Gy or 18 Gy WBR.

(E) H&E staining of the small intestine sections, magnification ×200.

1 (IGF-1), interleukin 11, keratinocyte growth factor (KGF), and fibroblast growth factor-2 (FGF-2), have been shown to protect crypt progenitor cells and increase animal survival following WBR, but their targets have not been identified (Booth and Potten, 2001). IGF-1, epidermal growth factor (EGF), and serum can suppress PUMA expression independent of p53 (Han et al., 2001; L.H. Ming, T. Sakaida, and J.Y, unpublished data). It is possible that inhibiting PUMA expression is a common mechanism underlying the radioprotective effects of these factors. If so, it might be useful to identify small molecule PUMA inhibitors with more desirable pharmacological properties. PUMA deficiency potently protects hematopoietic progenitor cells and lymphocytes from p53-dependent radiation-induced apoptosis (Erlacher et al., 2005; Wu et al., 2005). Since more than 50% of human tumors are defective in p53 (Vogelstein et al., 2000), it is expected that PUMA is not induced in these tumors following radiotherapy. Therefore, selectively curbing radiosensitivity in the normal tissues transiently by small molecule PUMA inhibitors might be particularly beneficial in cancer therapy.

EXPERIMENTAL PROCEDURES

Mice and Ionizing Radiation

The procedures of all animal experiments were approved by the Institutional Animal Care and Use Committee (IACUC) at University of Pittsburgh. The original *PUMA* KO mice on a mixed background (Jeffers et al., 2003) were backcrossed to C57BL/6 for six generations (F6). Eight- to ten-week-old $PUMA^{+/+}$ and $PUMA^{-/-}$ littermates were generated from F6 heterozygote breeding. C57BL/6 $p53^{-/-}$, $Bax^{-/-}$, and control mice were purchased from Jackson Laboratory. The mice were housed and genotypes as described (Wu et al., 2007). Mice were irradiated at doses ranging from 0 to 18 Gy at a rate of 82 cGy/min using a ^{137}Cs irradiator (Mark I, J.L. Shepherd and Associates, San Fernando, CA).

RNA In Situ Hybridization

The protocol has been previously described (Carson-Walter et al., 2005; St. Croix et al., 2000). Digoxygenin-labeled *PUMA* antisense RNA probes were generated by PCR amplification with incorporation of a T7 promoter into the antisense primer (Table S2).

Histological Analysis, TUNEL, and BrdU Staining

All mice were injected with BrdU (100 mg/kg; Sigma Chemical Co., St. Louis, MO) 2 hr prior to sacrifice. Sections (5 μm) from paraffin-embedded intestinal bundles were subjected to hematoxylin and eosin (H&E) staining for histological analysis.

TUNEL staining was performed using an ApopTag Kit (Chemicon international, Temecula, CA) according to the manufacturer's instructions. The apoptotic index was scored in full longitudinal sections of crypts containing at least 17 cells, including Paneth cells. The frequency of apoptosis for each cell position from the crypt bottom was scored in 200 half-crypt sections. Following BrdU staining, the BrdU-positive cells in the crypt were scored by counting 100 intact crypts. The data was reported as mean ± SEM. Three or more mice were used in each group. More detail protocols were described in the Supplemental Data.

Immunohistochemistry

The detailed methods for the staining of Musushi, Ki67, cryptdin 4, MMP-7, and double staining of TUNEL/CD105, TUNEL/MMP-7, *PUMA* ISH/TUNEL, *PUMA* ISH/MMP-7, *PUMA* ISH/CD105, and *PUMA* ISH/CD45 are described in the Supplemental Data.

Crypt Microcolony Assay

Stem cell survival was quantified by counting regenerated crypts in HE-stained and BrdU-stained cross-sections 4 days after radiation as detailed in the Supplemental Data. Four to five mice were used in each group, and the data were reported as means ± SEM.

Caspase 3 Activity Assay

The assay was performed as described using the extract of intestinal mucosal scraping, with the results expressed as absorbance at 405 nm per milligram protein (Wu et al., 2007). Each experiment was performed in triplicate and repeated at least twice. Six mice were used in each group.

Total RNA Extraction and Real-Time Reverse Transcriptase Polymerase Chain Reaction

Total RNA was prepared from freshly scraped mucosa, and cDNA was then generated for real-time PCR analysis of *PUMA* mRNA as described (Wu et al., 2007). Three mice were used in each group.

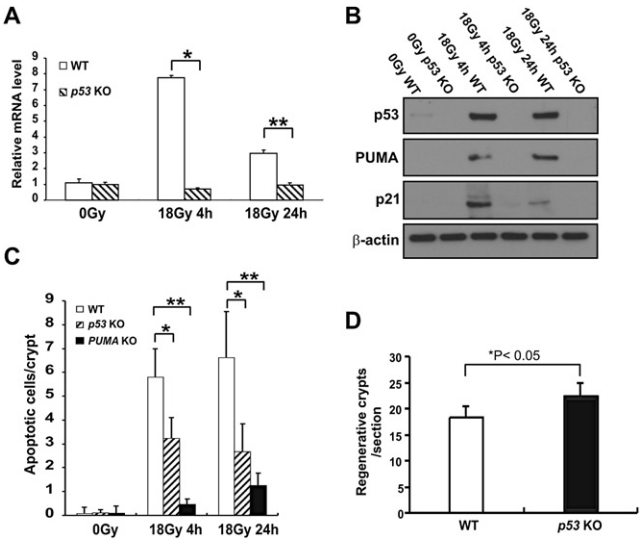

Figure 6. PUMA Mediated p53-Dependent Crypt Cell Apoptosis Induced by Radiation

(A) *PUMA* mRNA expression in the intestinal mucosa was evaluated by quantitative real-time RT-PCR. Values are means ± SD; n = 3 in each group. *p < 0.001; **p < 0.01.

(B) PUMA, p21, p53, and β-actin protein expression in the intestinal mucosa were determined by western blotting.

(C) Apoptotic index measured by TUNEL staining. Values are means ± SD, and n = 3 in each group. *p < 0.01, **p < 0.001.

(D) Regenerated crypts were quantitated after 15 Gy WBR by counting 10 BrdU stained sections. Values are means ± SD; n = 4 in each group.

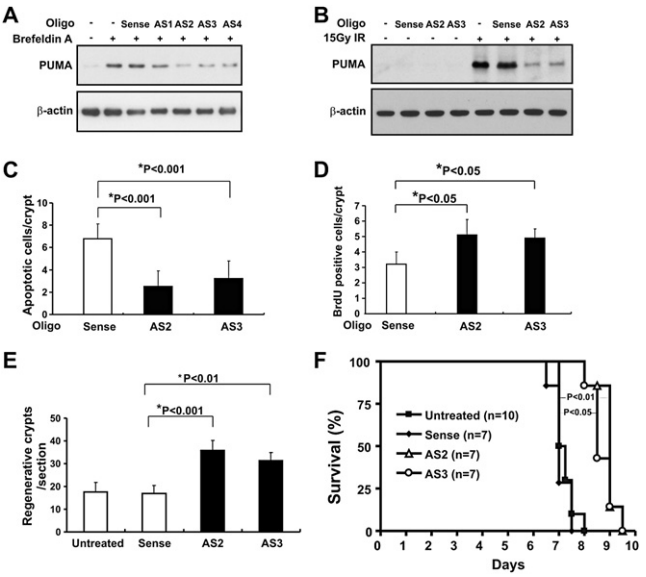

Figure 7. *PUMA* Antisense Oligonucleotides Suppressed Crypt Apoptosis and Prolonged Survival of Mice Following WBR

(A) The effects of *PUMA* antisense oligonucleotides on PUMA expression in MEFs after Brefeldin A (20 nM) treatment were evaluated by western blotting.

(B) PUMA expression in the small intestinal mucosa of mice treated with *PUMA* sense or antisense (AS) oligonucleotides at 24 hr following 15 Gy WBR.

(C and D) Apoptotic and BrdU incorporation indices in the crypt 24 hr after 15 Gy WBR. Values are means ± SD; n = 3 mice in each group.

(E) Crypt regeneration at 96 hr following 15 Gy WBR. Values are means ± SD; n = 5 mice in each group.

(F) Survival curves of mice following 15 Gy WBR.

Subcellular Fractionation and Western Blotting

Total protein extract, mitochondrial, and cytosolic fractions were purified and analyzed by NuPage gel (Invitrogen, Carlsbad, CA) electrophoresis as previously described (Kohli et al., 2004; Yu et al., 2003). The purified mitochondrial fractions were crosslinked using 1 mM Dithiobis(succinimidyl)propionate (DSP) (Pierce, Rockford, IL) to detect Bax or Bax multimerization as described (Wu et al., 2007). Three mice were used in each experimental group unless specified. The antibodies used were described in the Supplemental Data.

In Vitro and In Vivo Treatment with *PUMA* Antisense Oligonucleotide

Phosphorothioated *PUMA* antisense oligonucleotides AS1, AS2, AS3, and AS4 (Table S1) were synthesized by IDT (Coralville, IA). The MEFs (Sobol et al., 2003) were cultured in DMEM (Invitrogen) supplemented with 10% defined fetal bovine serum (Hyclone, Logan, UT), 100 units/ml penicillin and 100 μg/ml streptomycin (Invitrogen) The MEFs were treated with Brefeldin A (Calbiochem, La Jolla, CA) for 48 hr to test the efficiency of *PUMA* antisense oligos (12.5 μM). For in vivo studies, the mice were treated with *PUMA* sense or *PUMA* antisense oligo at 25 mg/kg/day via intraperitoneal (i.p.) injection, starting 2 days before WBR and continued until 4 days post-WBR. Seven to ten animals were used in each group for the survival studies.

Statistical Analysis

Data were analyzed by unpaired t test or ANOVA in which multiple comparisons were performed using the method of least significant difference. The survival data was analyzed by log-rank test using GraphPad Prism 4 software. Data in Figures 5A, 6D, and 7D were analyzed additionally by Mann-Whitney test, with the largest p value depicted. Differences were considered significant if the probability of the difference occurring by chance was less than 5 in 100 ($p < 0.05$).

SUPPLEMENTAL DATA

The Supplemental Data include two tables and ten figures and can be found with this article online at http://www.cellstemcell.com/cgi/content/full/2/6/576/DC1/.

ACKNOWLEDGMENTS

We thank other members of our laboratories for helpful discussion and comments. We thank Drs. Xiao-Ming Yin, Tao Cheng, Robert W. Sobol (University of Pittsburgh, Pittsburgh, PA), and Michael Selsted (University of California, Irvine, Irvine, CA) for Bid, CD45 antibodies, MEFs, and cryptdin 4 antiserum, respectively. We thank Dr. Yu Cheng (University of Pittsburgh) for help with statistical analysis and Drs. Linheng Li (Stowers Institute for Medical Research, Kansas City, MI) and Brad St. Croix (NCI, Fredrick, MD) for technical help with Musashi and CD105 IHC, respectively. This work was supported in part by Flight Attendant Medical Research Institute (FAMRI); the Alliance for Cancer Gene Therapy (ACGT) and UPCI Head and Neck SPORE Career Development Award (NIH, 1 P50 CA097190) (J.Y.); NIH grants CA106348 and CA121105; and American Cancer Society grant RSG-07-156-01-CNE (L.Z.). L.Z. is a V scholar.

Received: July 3, 2007
Revised: February 4, 2008
Accepted: March 13, 2008
Published: June 4, 2008

REFERENCES

Barker, N., van Es, J.H., Kuipers, J., Kujala, P., van den Born, M., Cozijnsen, M., Haegebarth, A., Korving, J., Begthel, H., Peters, P.J., and Clevers, H.

(2007). Identification of stem cells in small intestine and colon by marker gene Lgr5. Nature *449*, 1003–1007.

Booth, D., and Potten, C.S. (2001). Protection against mucosal injury by growth factors and cytokines. J. Natl. Cancer Inst. Monogr. *29*, 16–20.

Carson-Walter, E.B., Hampton, J., Shue, E., Geynisman, D.M., Pillai, P.K., Sathanoori, R., Madden, S.L., Hamilton, R.L., and Walter, K.A. (2005). Plasmalemmal vesicle associated protein-1 is a novel marker implicated in brain tumor angiogenesis. Clin. Cancer Res. *11*, 7643–7650.

Ch'ang, H.J., Maj, J.G., Paris, F., Xing, H.R., Zhang, J., Truman, J.P., Cardon-Cardo, C., Haimovitz-Friedman, A., Kolesnick, R., and Fuks, Z. (2005). ATM regulates target switching to escalating doses of radiation in the intestines. Nat. Med. *11*, 484–490.

Erlacher, M., Michalak, E.M., Kelly, P.N., Labi, V., Niederegger, H., Coultas, L., Adams, J.M., Strasser, A., and Villunger, A. (2005). BH3-only proteins Puma and Bim are rate-limiting for gamma-radiation- and glucocorticoid-induced apoptosis of lymphoid cells in vivo. Blood *106*, 4131–4138.

Ge, A.Z., and Butcher, E.C. (1994). Cloning and expression of a cDNA encoding mouse endoglin, an endothelial cell TGF-beta ligand. Gene *138*, 201–206.

Giannakis, M., Stappenbeck, T.S., Mills, J.C., Leip, D.G., Lovett, M., Clifton, S.W., Ippolito, J.E., Glasscock, J.I., Arumugam, M., Brent, M.R., and Gordon, J.I. (2006). Molecular properties of adult mouse gastric and intestinal epithelial progenitors in their niches. J. Biol. Chem. *281*, 11292–11300.

Gudkov, A.V., and Komarova, E.A. (2003). The role of p53 in determining sensitivity to radiotherapy. Nat. Rev. Cancer *3*, 117–129.

Han, J., Flemington, C., Houghton, A.B., Gu, Z., Zambetti, G.P., Lutz, R.J., Zhu, L., and Chittenden, T. (2001). Expression of bbc3, a pro-apoptotic BH3-only gene, is regulated by diverse cell death and survival signals. Proc. Natl. Acad. Sci. USA *98*, 11318–11323.

He, X.C., Yin, T., Grindley, J.C., Tian, Q., Sato, T., Tao, W.A., Dirisina, R., Porter-Westpfahl, K.S., Hembree, M., Johnson, T., et al. (2007). PTEN-deficient intestinal stem cells initiate intestinal polyposis. Nat. Genet. *39*, 189–198.

Hendry, J.H., Booth, C., and Potten, C.S. (2001). Endothelial cells and radiation gastrointestinal syndrome. Science *294*, 1411.

Jeffers, J.R., Parganas, E., Lee, Y., Yang, C., Wang, J., Brennan, J., MacLean, K.H., Han, J., Chittenden, T., Ihle, J.N., et al. (2003). Puma is an essential mediator of p53-dependent and -independent apoptotic pathways. Cancer Cell *4*, 321–328.

Kohli, M., Yu, J., Seaman, C., Bardelli, A., Kinzler, K.W., Vogelstein, B., Lengauer, C., and Zhang, L. (2004). SMAC/Diablo-dependent apoptosis induced by nonsteroidal antiinflammatory drugs (NSAIDs) in colon cancer cells. Proc. Natl. Acad. Sci. USA *101*, 16897–16902.

Komarova, E.A., Kondratov, R.V., Wang, K., Christov, K., Golovkina, T.V., Goldblum, J.R., and Gudkov, A.V. (2004). Dual effect of p53 on radiation sensitivity in vivo: p53 promotes hematopoietic injury, but protects from gastrointestinal syndrome in mice. Oncogene *23*, 3265–3271.

Merritt, A.J., Potten, C.S., Kemp, C.J., Hickman, J.A., Balmain, A., Lane, D.P., and Hall, P.A. (1994). The role of p53 in spontaneous and radiation-induced apoptosis in the gastrointestinal tract of normal and p53-deficient mice. Cancer Res. *54*, 614–617.

Ming, L., Wang, P., Bank, A., Yu, J., and Zhang, L. (2006). PUMA dissociates Bax and BCL-XL to induce apoptosis in colon cancer cells. J. Biol. Chem. *281*, 16034–16042.

Nakano, K., and Vousden, K.H. (2001). PUMA, a novel proapoptotic gene, is induced by p53. Mol. Cell *7*, 683–694.

Paris, F., Fuks, Z., Kang, A., Capodieci, P., Juan, G., Ehleiter, D., Haimovitz-Friedman, A., Cordon-Cardo, C., and Kolesnick, R. (2001). Endothelial apoptosis as the primary lesion initiating intestinal radiation damage in mice. Science *293*, 293–297.

Potten, C.S. (2004). Radiation, the ideal cytotoxic agent for studying the cell biology of tissues such as the small intestine. Radiat. Res. *161*, 123–136.

Potten, C.S., Booth, C., Tudor, G.L., Booth, D., Brady, G., Hurley, P., Ashton, G., Clarke, R., Sakakibara, S., and Okano, H. (2003). Identification of a putative intestinal stem cell and early lineage marker; musashi-1. Differentiation *71*, 28–41.

Sobol, R.W., Kartalou, M., Almeida, K.H., Joyce, D.F., Engelward, B.P., Horton, J.K., Prasad, R., Samson, L.D., and Wilson, S.H. (2003). Base excision repair intermediates induce p53-independent cytotoxic and genotoxic responses. J. Biol. Chem. *278*, 39951–39959.

St. Croix, B., Rago, C., Velculescu, V., Traverso, G., Romans, K.E., Montgomery, E., Lal, A., Riggins, G.J., Lengauer, C., Vogelstein, B., and Kinzler, K.W. (2000). Genes expressed in human tumor endothelium. Science *289*, 1197–1202.

Stappenbeck, T.S., Mills, J.C., and Gordon, J.I. (2003). Molecular features of adult mouse small intestinal epithelial progenitors. Proc. Natl. Acad. Sci. USA *100*, 1004–1009.

Strasser, A., Harris, A.W., Jacks, T., and Cory, S. (1994). DNA damage can induce apoptosis in proliferating lymphoid cells via p53-independent mechanisms inhibitable by Bcl-2. Cell *79*, 329–339.

Suit, H.D., and Withers, H.R. (2001). Endothelial cells and radiation gastrointestinal syndrome. Science *294*, 1411.

Villunger, A., Michalak, E.M., Coultas, L., Mullauer, F., Bock, G., Ausserlechner, M.J., Adams, J.M., and Strasser, A. (2003). p53- and Drug-Induced Apoptotic Responses Mediated by BH3-Only Proteins Puma and Noxa. Science *302*, 1036–1038.

Vogelstein, B., Lane, D., and Levine, A.J. (2000). Surfing the p53 network. Nature *408*, 307–310.

Wang, P., Yu, J., and Zhang, L. (2007). The nuclear function of p53 is required for PUMA-mediated apoptosis induced by DNA damage. Proc. Natl. Acad. Sci. USA *104*, 4054–4059.

Wu, B., Qiu, W., Wang, P., Yu, H., Cheng, T., Zambetti, G.P., Zhang, L., and Yu, J. (2007). p53 independent induction of PUMA mediates intestinal apoptosis in response to ischaemia-reperfusion. Gut *56*, 645–654.

Wu, W.S., Heinrichs, S., Xu, D., Garrison, S.P., Zambetti, G.P., Adams, J.M., and Look, A.T. (2005). Slug antagonizes p53-mediated apoptosis of hematopoietic progenitors by repressing puma. Cell *123*, 641–653.

Yu, J., and Zhang, L. (2005). The transcriptional targets of p53 in apoptosis control. Biochem. Biophys. Res. Commun. *331*, 851–858.

Yu, J., Zhang, L., Hwang, P.M., Kinzler, K.W., and Vogelstein, B. (2001). PUMA induces the rapid apoptosis of colorectal cancer cells. Mol. Cell *7*, 673–682.

Yu, J., Wang, Z., Kinzler, K.W., Vogelstein, B., and Zhang, L. (2003). PUMA mediates the apoptotic response to p53 in colorectal cancer cells. Proc. Natl. Acad. Sci. USA *100*, 1931–1936.

Yu, J., Wang, P., Ming, L., Wood, M.A., and Zhang, L. (2007). SMAC/Diablo mediates the proapoptotic function of PUMA by regulating PUMA-induced mitochondrial events. Oncogene *26*, 4189–4198.

Zong, W.X., Lindsten, T., Ross, A.J., MacGregor, G.R., and Thompson, C.B. (2001). BH3-only proteins that bind pro-survival Bcl-2 family members fail to induce apoptosis in the absence of Bax and Bak. Genes Dev. *15*, 1481–1486.